30th International Conference
ENGINEERING MECHANICS 2024
Milovy, Czech Republic, May 14 – 16, 2024

INFLUENCE OF ARTERY UNFOLDMENT ON ITS MECHANICAL RESPONSE

Sochor O.*, Hrubanová A., Joukal M.***, Burša J.‡**

Abstract: *This study investigates the influence of artery unfoldment on its mechanical response in planar tension test. Inflation test was chosen for comparison because, with the axial stretch $\lambda_z = 1$, it also keeps plane strain condition. Both tests were simulated in silico using finite element method. The geometry models correspond to aorta and common carotid artery with distinguished two layers within the arterial wall; a homogenous wall model was also used for comparison. Material models were acquired by fitting the uniaxial tension tests of human carotid arteries dissected into media and adventitia layers with 3rd order Yeoh hyperelastic model. The results showed that the artery segment straightening leads to a non-uniform stress distribution throughout the specimen thickness with the maximum stress located at the inner surface of the artery. By comparing stresses (averaged throughout the thickness) at specified strain levels up to 30 %, the influence of specimen unfoldment was estimated with inflation test taken as a basis. For the carotid artery, stresses in the planar tension test were higher by 27−61 % while for the aorta the difference was between 8 and 17 %. The difference between individual arteries occurs due to the varying thickness-to-radius ratio.*

Keywords: Tension test, inflation test, finite element simulation, unfoldment, arterial wall.

1. Introduction

For 2019 the World Health Organization reported that one-third of all deaths were caused by diseases associated with the cardiovascular system (WHO, 2020). The leading causes were heart attack and stroke, both resulting dominantly from atherosclerotic plaque rupture and consequent thrombus formation. Thrombus can embolize and plug smaller blood vessel, resulting in the previously mentioned diseases. The main course in recent years leads to evaluation of the risk of plaque rupture using biomechanical modelling (Gholipour et al., 2018). Here the knowledge of geometry, loading conditions and material characteristics is crucial. Various mechanical tests such as uniaxial (Lisický et al., 2021) or equibiaxial (Polzer et al., 2015).

	Parameters	Carotid model	Aorta model
Inner radius [mm]	R_i	2.9	7.9
Media thickness [mm]	T_M	0.72	0.88
Adventitia thickness [mm]	T_A	0.37	0.41
Artery length [mm]	L	10	10

Tab. 1: Geometry parameters.

* Ing. Ondřej Sochor: Inst. Solid Mechanics, Mechatronics and Biomechanics, Brno University of Technology, Technická 2896/2; 616 69, Brno; CZ, 209128@vutbr.cz

** Ing. Anna Hrubanová: Inst. Solid Mechanics, Mechatronics and Biomechanics, Brno University of Technology, Technická 2896/2; 616 69, Brno; CZ

*** Assoc. Prof. MUDr. Marek Joukal, PhD.: Department of Anatomy, Faculty of Medicine, Masaryk University, Kamenice 126/3; 625 00, Brno; CZ

‡ Prof. Ing. Jiří Burša, PhD.: Inst. Solid Mechanics, Mechatronics and Biomechanics, Brno University of Technology, Technická 2896/2; 616 69, Brno; CZ

doi: 10.21495/em2024-274

tension tests, planar tension test (Cunnane et al., 2016), or inflation tests (Sommer et al., 2010) are used to obtain artery wall response. Except for the last one, the specimens must be axially cut and unfolded to obtain response in the circumferential direction. However, this unfoldment leads to a certain pre-strain before testing, which might influence the mechanical response of artery tissue. The aim of this study is to analyze the influence of artery segment straightening on its mechanical response in the planar tension tests, using finite element simulations.

2. Material and methods

2.1. Geometry models

To analyze the effect of unfoldment on mechanical testing, simulations of a planar tension test and an inflation test were performed. These tests evoke the same stress/strain states if the axial stretch of the cylinder specimen is kept at $\lambda_z = 1$. For both simulations, a bilayer model and a homogeneous model were used. To simulate the planar tension test, a 2D plane strain model of a closed (unloaded) artery was employed (Fig. 1 left), with one end fixed and the other end rotated and shifted to obtain an unfolded (planar) configuration. In the second loadstep, its stretch was simulated by displacement condition in the x-axis. Regarding simulation of the inflation test, a 2D axisymmetric model of a cylindrical artery was used (see Fig. 1 right). To prevent axial (y-axis) deformation, a zero-displacement condition in axial direction on both ends was used. A 0.20 MPa pressure was applied on the inner surface of the model. Geometry characteristics of both models are summarized in Tab. 1; those of thoracic aorta were taken from (Holzapfel et al., 2007); those of carotid were measured during specimen preparation. Mesh sensitivity analysis was done, resulting in 4 400 quadratic elements for each model. Each loadstep was divided into 100 substeps to obtain a dense response curve.

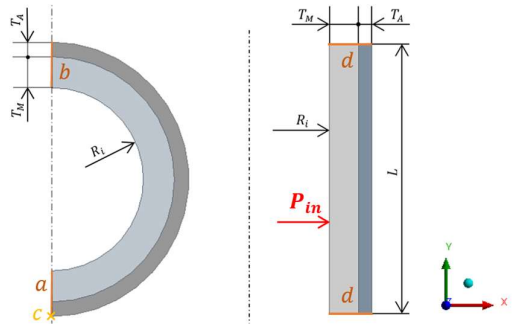

Fig. 1: Geometry models and boundary conditions for each test:
Left: planar tension test – model before unfoldment. Loads: a: UX = 0 mm; c: fixed support; b: remote rigid displacement, rotZ = -180 (in the first loadstep), UX = 16 mm (in the second loadstep),
Right: inflation test – cylindrical model, loads: d: UY = 0, p_{in} = 0.20 MPa.

2.2. Mechanical testing

Three samples of non-pathological carotid artery from human cadavers (age 88, 77, 83) were excised during autopsy at Masaryk University, Department of Pathology. Fresh samples were immersed in 0.9 % saline solution and kept frozen at -20 °C. Before testing the samples were thawed and the artery was carefully separated into adventitia and media layers. In total, 10 rings with average width of 3 mm were obtained for each layer. Each ring was cut axially and the created specimen was clamped in a tensile tester (Camea s.r.o., Czech Republic). A pre-load of 0.01 N was applied to straighten the specimen (in saline bath at 37 °C) and then load was increased till rupture (Lisický et al., 2021).

2.2. Constitutive models

For each layer the obtained stress-strain curves were averaged at specified stress levels and then fitted with hyperelastic incompressible 3rd order Yeoh model (Yeoh, 1993) using Hyperfit software (www.hyperfit.wz.cz). The resulting material parameters are summarized in Tab. 2.

To acquire material parameters for the homogeneous wall, which was not tested, a simulation of uniaxial tension test of the bilayer wall was performed in Ansys Workbench 2023 R2 with the mean thickness

0.78 mm (media) and 0.34 mm (adventitia) measured during the tension tests. The response of each material model is shown in Fig. 2.

Material constants	Media	Adventitia	Homogeneous
C_{10} [kPa]	44.9	67.9	53.0
C_{20} [kPa]	1 102.7	2 155.6	1 469.2
C_{30} [kPa]	0	0	29.1

Tab. 2: Material constants for Yeoh model.

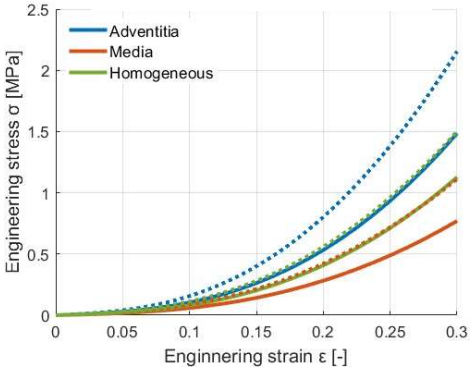

Fig. 2: Uniaxial tension curves of the models: solid lines - uniaxial tension, dotted - planar tension.

3. Results

First, the x-axis stresses/strains of the unfolded models were evaluated. The transmural stress distribution of unfolded bilayer model after the second load step, i.e. end of plane tension (Fig. 3a) was obtained.

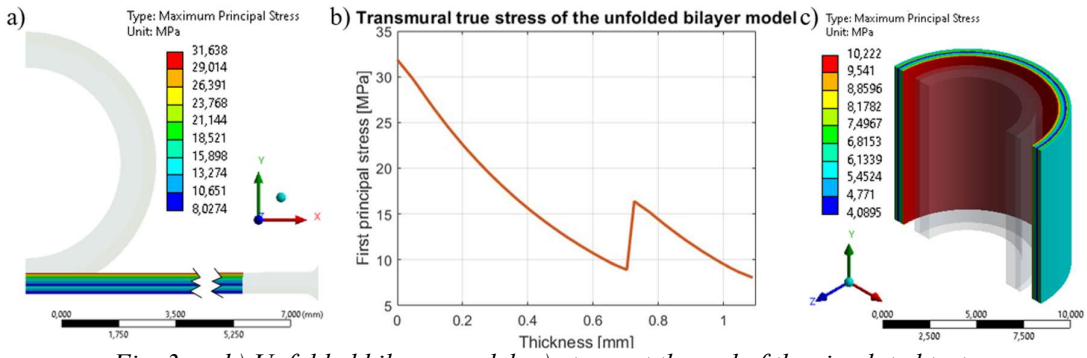

Fig. 3: a–b) Unfolded bilayer model, a) stress at the end of the simulated test, b) transmural stress; 0 mm - inner edge of media, c) cylindrical model after inflation.

As a stress singularity occurred at the free end of the unfolded model (due to the remote displacement condition with rigid behavior), this area was excluded from evaluation. The unfolded (originally half cylindrical) model was bended after the first load-step, thus a linear distribution of stress throughout the wall thickness occurred, with maximum and minimum stresses situated at the inner and outer edges of the model, respectively. At the end of test, the stress distribution decreases from the inner edge of media (global maximum) to the media's outer edge (Fig. 3b). A second local maximum occurs at the inner edge of adventitia. For the homogeneous wall, the stress decreases monotonously with distance from the inner edge. For the cylindrical models under inflation, the first principal stresses were evaluated (see Fig. 3c); their

	Carotid	Aorta
$\varepsilon_{0.10}$	61.4 %	16.9 %
$\varepsilon_{0.20}$	36.8 %	8.3 %
$\varepsilon_{0.30}$	27.5 %	8.3 %

Tab. 3: Percentual stress differences between the unfolded and cylindrical bilayer models for both arteries at strain levels of 10, 20 and 30 %.

transmural trends were the same as for the unfolded model. For each model, the average values of engineering stresses/strains throughout the specimen thickness were calculated. For plotted stress-strain curves see Fig. 4.

To estimate the influence of unfoldment on stress-strain curves of each artery, differences between the bilayer unfolded and cylinder models were calculated at three strain levels (in percentage, with the cylindrical model considered as a basis, see Tab. 3).

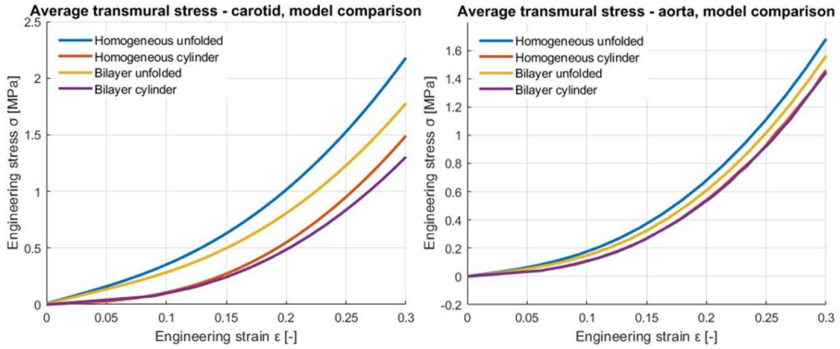

Fig. 4: Averaged stress/strain characteristics for different models.

4. Discussion and conclusion

The obtained results indicate that the specimen unfoldment significantly influences the plane strain tension tests of carotid arteries (Fig. 4), with differences reaching more than 60 % (Tab. 3). The unfoldment leads to non-uniform transmural distribution of stress, resulting in maximum stress occurring at the inner edge of the carotid artery. Due to the pronounced stiffening response of the artery tissues, the maximum stresses at the inner surface of the artery dominate the response, resulting in a more than 60 % increase of the initial stiffness. Similarly, the initial stiffness of the aorta is also increased, but by 17 % only. This difference between both arteries is given by their very different thickness-to-radius ratio (0.38 for carotid artery and 0.16 for aorta) and decreases with increasing strains. These numerical results, however, relate not only to the specific geometric parameters but also to the material properties of the investigated arteries and do not consider residual stresses. While the axial pre-stress is negligible due to the high age of donors, the circumferential component may be significant. For a positive opening angle being a typical representation of these residual stresses, they are negative on the inner surface and thus could reduce the presented effect. Due to lack of experimental data, however, this is out of scope of this paper. Thus, the impact of unfoldment on the stress-strain responses should be assessed individually for each investigated artery and ideally with exploitation of its specific material properties and opening angles.

Acknowledgements

This work was supported by Czech Science Foundation, project No. 21-21935S.

References

Cunnane, E. M. et al. (2016) Mechanical properties and composition of carotid and femoral atherosclerotic plaques: A comparative study. *J Biomech*, 49 (15), 3697–3704.

Gholipour, A. et al. (2018) Three-dimensional biomechanics of coronary arteries. *Int J Engin Sci*, 130, 93–114.

Holzapfel, G. A. et al. (2007) Layer-specific 3D residual deformations of human aortas with non-atherosclerotic intimal thickening. *Annals of biomedical engineering*, 35(4), 530–545.

Lisický, O., Hrubanová, A., Staffa, R., Vlachovský, R. and Burša, J. (2021) Constitutive models and failure properties of fibrous tissues of carotid artery atheroma based on their uniaxial testing. *J Biomech.*, 129, 110861–110861.

Polzer, S., Gasser T. C., Novák K., Man V., Tichy M., Skacel P. and Bursa J (2015) Structure-based constitutive model can accurately predict planar biaxial properties of aortic wall tissue. *Acta Biomaterialia*, 14, 133–145.

Sommer, G. et al. (2010) Biaxial mechanical properties of intact and layer-dissected human carotid arteries at physiological and supraphysiological loadings. *Am J Physio Heart Circ Physiol*, 298(3), H898–H912.

Yeoh, O. H. (1993) Some forms of the strain energy function for rubber. *Rubber Chemistry and Technology*, 754–771.

World Health Organization (2020) The top 10 causes of death. from https://www.who.int/news-room/fact-sheets/detail/the-top-10-causes-of-death.